Frozen-core model of the double photoionization of beryllium

A. S. Kheifets

Research School of Physical Sciences,

*The Australian National University, Canberra ACT 0200, Australia**

Igor Bray

Centre for Atomic, Molecular, and Surface Physics,

School of Mathematical and Physical Sciences,

Murdoch University, Perth, 6150 Australia †

(Dated: July 4, 2001)

Abstract

We calculate the ionization-exitation and double ionization cross-sections of the valence $2s^2$ shell of beryllium. Our model combines a multiconfiguration Hartree-Fock expansion of the beryllium atom ground state and a momentum space close-coupling expansion of the final ionized state. A near-complete set of negative and positive energy pseudostates is employed to represnet various singly and doubly ionized channels. The role of the frozen $1s^2$ core is elucidated by comparing the beryllium single and double photoionization cross-sections with those of the "hollow" helium $2s^2$ atom in which the $2s$ orbital is made orthogonal to the vacant $1s$ orbital. The angular correlation in the two-electron continuum is studied by calculating the triply differential cross-section of Be at equal energy sharing between the photoelectrons.

*Electronic address: A.Kheifets@anu.edu.au; URL: http://rsphysse.anu.edu.au/~ask107

†Electronic address: I.Bray@murdoch.edu.au; URL: http://yin.ph.flinders.edu.au/igor.html

I. INTRODUCTION

Two-electron single-photon ionization processes including ionization with excitation (exitation-photoionization - EPI) and double photoionization (DPI) are only possible due to many-electron correlations. As such, these processes constitute an ideal testing ground for various theoretical models dealing with correlations. Most of the experimental and theoretical studies of the two-electron photoionization have been peroformed so far on He. The helium atom is the simplest two-electron target with no relevant structure of the remaining He^{2+} ion. This simplifies considerably theoretical treatment and interpretation of experimental results. Other members of the helium isoelectronic sequence (H^-, Li^+ etc) can be treated with the same level of accuracy. However, these targets are difficult to handle experimentally.

There is another class of atomic targets, namely the alkaline-earth atoms, which can be treated, in some approximation, as two-electron systems. Indeed, a compact electron core is well separated, both in the corrdinate space and in energy, from the valence ns^2 shell. At relatively small photon energies the inner core electrons can be treated as "spectators" not taking a direct part in the photoionization of the outer valence electrons. In this case the influence of the core on the valence electrons can be included via the self-consistent field and/or the polarization potential. This scheme is implemented to describe the single-photon one-electron photoionization of the valence shell in Be, Mg and Ca.

Several attempts have been made to study the two-electron ionization in the alkaline-earth atoms. The fully-resolved triple differential cross-section (TDCS) of the DPI of Ca have been measured in the region of the giant $3p-3d$ resonance [1, 2]. These measurements have been analyzed in subsequent theoretical papers [3–5]. However, a complete theory of the DPI in the resonance region is still lacking because of a complex nature of this process. Resonance-free DPI in Ca has been measured very recently [6] and this new set of data awaits its theoretical interpetation.

Double ionization of Mg by electron impact has been studied by the Maryland group with the view of obtaining the two-electron momentum density [7]. Experiments on the direct and resonant DPI of Be and Mg are now underway at the Photon Factory [8]. Theoretical interpretation of the Be measurements will be the most straightforward since the valence $2s^2$ is very well separated from the $1s^2$ core. Accordingly, there is good motivation for studying

the problem from a theoretical perspective. Here, we complement the study by Colgan and Pindzola, who used the time-dependent close-coupling approach at a few energies [9], by a systematic study on a broad energy range using the convergent close-coupling (CCC) method.

In our earlier works [10, 11] we applied the CCC method to describe the two-electron photoionization of the helium atom and its isoelectronic sequence. In this method the two-electron photoionization is treated as a two-stage process. The single photoionization is followed by scattering of the photoelectron on the positive ion thus producing various singly ionized and excited as well as the doubly ionized final states. By employing the Hylleraas or multiconfiguration Hartree-Fock (MCHF) ground state wave functions, the CCC method provides a very accurate description of both the total and the fully-differential photoionization cross-sections, independent of the gauge of the electromagnetic operator.

Here we report an application of the same theoretical scheme to the two-electron photoionization of the valence $2s^2$ shell of the beryllium atom. The static ground state correlation in this shell is described by employing a MCHF wave function in which the $1s^2$ core is frozen. The dynamic correlation in the two-electron continuum is represented by a momentum space close-coupling expansion, obtained from a CCC calculation for electron-impact ionization of Be^+. The target space is spanned by a set of negative and positive energy pseudostates which diagonlize the Hamiltonian of the positive Be^+ ion. The lowest, in energy, target state represents the frozen atomic core ($1s^2$ in the case of beryllium). The photoelectron wave function is calculated in the Hartree-Fock field of this frozen core.

To elucidate the role of the frozen core we calculate the two-electron photoionization of a simpler target in which the $1s^2$ shell screens the $Z = 4$ charge of Be to the $Z = 2$ of He. We call the resulting system the "hollow" $2s^2$ helium. Unlike the autoionizing $2s^2$ state of the real helium atom, in the "hollow" helium the $2s$ state is made orthogonal to the missing $1s^2$ shell.

In addition to the total cross-sections of the two-electron photoionization we also calculate the triply differential double photoionization cross-section at equal energy sharing between the photoelectrons. We apply a Gaussian ansatz to the squared double photoionization aplitude (correlation factor) and compare the Gaussian width parameters of the Be and He atoms.

The rest of the paper is organized as follows. In the next section we give a detailed

description of the MCHF ground states of Be and "hollow" He. In Section III we present the CCC formalism as applied to the frozen-core beryllium. Section IV contains our results for the total and differential photoionization cross-sections.

II. MCHF GROUND STATE

We assume the LS coupling scheme and make the following configuration-interaction expansion of the ^1S ground state:

$$\Psi_0(\boldsymbol{r}_1, \boldsymbol{r}_2) = \sum_{nl} C_{nl} \, |\phi_{nl}(\boldsymbol{r}_1) \, \phi_{nl}(\boldsymbol{r}_2) \; :^1S\rangle \tag{1}$$

Only diagonal nl^2 terms are included in (1) as is always the case for the MCHF ground state. This is so because a HF ground state is stable with respect to the one-electron-one-hole exitations and the first non-vanishing correction should be of the two-electron-two-hole type.

The coefficients in the MCHF expansion (1) are found by using the MCHF computer code [12]. The number of terms in the MCHF expansion is increasing until we are satisfied with the accuracy in terms of the energy and, more importantly, the asymptotic EPI and DPI ratios. As was shown by Dalgarno and Stewart [13] these ratios can be calculated solely from the ground state wave function through the overlap integrals

$$c_n \propto \left| \langle \phi^+_{ns} | \, \delta(\boldsymbol{r}_2) \, | \, \Psi_0 \rangle \right|^2 \quad , \quad c \propto |\langle \Psi_0 | \, \delta(\boldsymbol{r}_2) | \Psi_0 \rangle|^2 \tag{2}$$

In the above expression ϕ^+_{ns} is the one-electron ns orbital of the singly ionized atom. The asymptotic DPI and EPI ratios are then given by,

$$R^\infty_n = \left. \frac{\sigma_n}{\sigma^+ + \sigma^{++}} \right|_{\omega\to\infty} = \frac{c_n}{c} \quad , \quad R^\infty = \left. \frac{\sigma^{++}}{\sigma^+} \right|_{\omega\to\infty} = \frac{c - \sum_n c_n}{\sum_n c_n} \, , \tag{3}$$

where σ_n is the partial EPI cross-section, and $\sigma^+ = \sum_{n=1}^\infty \sigma_n$ and σ^{++} are the total single and double photoionization cross-sections. Here we follow notations of Refs. [14, 15] and define R_n as the ratio of the partial to the *total* cross-sections whereas R is defined as the ratio of the double to *single* cross-sections. Results for R^∞_n and R^∞ are shown in the Table. For comparison, we also show the corresponding results for the ground state He and the "hollow" $2s$ helium in which the $2s$ orbital is made orthogonal to the missing $1s$ orbital. The asymptotic photoionization cross-section ratios are quite close for Be and the hollow

He. In the following sections we will see that other photoionization results are also quite close for these two targets. This indicates a relatively minor role played by the frozen $1s^2$ core in the two-electron photoionization of the valence $2s^2$ shell of Be.

III. CCC FORMALISM

The photoionization cross section, as a function of the photon energy ω, corresponding to a particular bound electron state j of the ionized target is given by [16]

$$\sigma_j(\omega) \;=\; \frac{4\pi^2}{\omega c}\sum_{m_j}\int d^3k_b\,|\langle\Psi_j^{(-)}(\boldsymbol{k}_b)\,|\mathcal{D}|\,\Psi_0\rangle|^2\,\delta(\omega-E+E_0), \tag{4}$$

where $c\simeq 137$ is the speed of light in atomic units.

The dipole electro-magnetic operator $\mathcal{D}$ can be written in one of the following forms commonly known as length, velocity and acceleration:

$$\begin{aligned}\mathcal{D}^r &= \omega(z_1+z_2)\\ \mathcal{D}^\nabla &= \nabla_{z_1}+\nabla_{z_2}\\ \mathcal{D}^{\dot\nabla} &= \frac{Z}{\omega}\left(\frac{z_1}{r_1^3}+\frac{z_2}{r_2^3}\right),\end{aligned} \tag{5}$$

with the z axis chosen along the polarization vector of the photon. We used all the three gauges in our previous calculations on He [10, 11, 17]. However, the acceleration gauge cannot be used with the presently emploed frozen core model. This gauge enhances the small distances from the nucleus where the excitations from the core $1s^2$ shell are important. This excitations cannot be accounted for in the frozen-core model.

The dipole matrix element entering Eq. (5) is calculated as

$$\begin{aligned}\langle\Psi_j^{(-)}(\boldsymbol{k}_b)|\mathcal{D}|\Psi_0\rangle \;=\; &\langle\boldsymbol{k}_b^{(-)}j|\mathcal{D}|\Psi_0\rangle\\ &+\sum_i\sum\!\!\!\!\!\!\int d^3k\frac{\langle\boldsymbol{k}_b^{(-)}j|T|i\boldsymbol{k}^{(+)}\rangle\langle\boldsymbol{k}^{(+)}i\,|\mathcal{D}|\,\Psi_0\rangle}{E-\varepsilon_{\boldsymbol{k}}-\epsilon_i+i0}.\end{aligned} \tag{6}$$

Here the channel wavefunction $\langle\boldsymbol{k}_b^{(-)}j|$ is the product of a one-electron target orbital φ_j with energy ϵ_j and a (distorted) Coulomb outgoing wave $\chi^{(-)}(\boldsymbol{k}_b)$ with energy $\varepsilon_{\boldsymbol{k}}$. Like in the case of helium, the target orbital is generated with the asymptotic charge being two, and the asymptotic charge seen by the Coulomb wave is one.

The square-integrable basis set of the target states ϕ_n^N is obtained by diagonalizing the target Hamiltonian H_T in a large Laguerre (Sturmian) basis of size N

$$\langle \varphi_m^N | H_T | \varphi_n^N \rangle = \epsilon_n^N \delta_{mn}. \tag{7}$$

The target Hamiltonian is defined as

$$H_T = \sum_{i=1}^{Z} (K_i + V_i) = \sum_{i=1}^{Z} \left(-\frac{1}{2}\nabla_i^2 + V_i^{\rm FC} + V_i^{\rm pol} \right) \tag{8}$$

The non-local frozen-core Hartree-Fock potential $V^{\rm FC}$ is generated by performing a self-consistent-field Hartree-Fock calculation [18] for the ground state of the Be^{2+} ion

$$V^{\rm FC}\varphi_\alpha(\boldsymbol{r}) = \left(-\frac{Z}{r} + 2 \sum_{\varphi_j \in C} \int d^3r' \frac{|\, \varphi_j(\boldsymbol{r'}) \,|^2}{|\, \boldsymbol{r} - \boldsymbol{r'} \,|} \right) \varphi_\alpha(\boldsymbol{r}) - \sum_{\varphi_j \in C} \int d^3r' \frac{\varphi_j^*(\boldsymbol{r'})\varphi_\alpha(\boldsymbol{r'})}{|\, \boldsymbol{r} - \boldsymbol{r'} \,|} \varphi_j(\boldsymbol{r}), \tag{9}$$

Polarization potential

$$V^{\rm pol}(r) = -\alpha_d / 2r^4 \; W_6(r/\rho),$$

where

$$W_m(r/\rho) = \{1 - \exp\left[-(r/\rho)^m\right]\},$$

and α_d is the static dipole polarizability of the core. For the case of the Be^+ ion there is no need to use $V^{\rm pol}$, and so we set $\alpha_d = 0$. However, the polarization potential would have to be included for heavier atoms like Mg and Ca.

The contribution from the final channels $\langle \boldsymbol{k}_b^{(-)} j|$ is separated into single and double ionization according to the energy of the ϵ_j which are positive for the double ionized channels and negative for the singly ionized channels. We also ensure that for the negative-energy state cross sections, contributions to the ionization plus excitation cross sections are multiplied by the projection of the state onto the true target discrete subspace as is done for electron-impact ionization [19]. The fully differential DPI TDCS is calculated from the same dipole matrix element (5), but without integration over the momentum of the one photoelectron. Details of the TDCS calculation are presented elsewhere [20].

The number of the states N in the Laguerre basis (7) was increased until satisfactory convergence is achieved. In practice, our calculations were performed with $20 - l$ target states where $l = 0, \ldots, l_{\rm max}$ is the angular momentum of the target orbital and $l_{\rm max} = 5$. Higher values of the $l_{\rm max}$ are required for Be than for He because of a larger radial extent of the target orbitals. To get convergence in the TDCS even higher $l_{\rm max} = 7$ was necessary.

IV. RESULTS

A. Total EPI and DPI cross-sections

We test our model by first calculating the ground state single photoionization cross-section. This cross-section corresponds to the Be^+ ion being left in its ground state $2s^1$. Our results in the length and velocity forms are shown in Fig. 1. In the same figure we also show the calculations of Radoević and Johnson [21] (labeled as RJ) in the random phase approximation with exchange (RPAE) and the Tamm-Dancoff approximation (TD). These calculations are available in a smaller photon energy range closer to the single ioonization threshold. Where a comparison can be made, our results are close to those of Radoević and Johnson.

A more complex truly two-electron process is the ionization with excitation in which the Be^+ ion is left in an excited state $nl, n > 2$. We show our results for the ionization-excitation in Fig. 2 in the form of the cross-section ratios $R_n = \sigma_n/(\sigma^+ + \sigma^{++})$ for $n = 3 \ldots 6$. The asymptotica ratios R_n^∞ calculated according to formula (3) and listed in the Table are indicated by the arrows. The cross-section ratios flatten at photon energy above 200 eV and approach quite closely the asymptotic values. Of course, one should bear in mind that the frozen core model is most accurate at photon energies below the third ionization potential, i.e. below 180 eV for Be. So, approaching a correct asymptotic limit only indicates an internal consistency of our model.

In the same figure we show analogous ratios calculated for the "hollow" helium. Calculation for the velocity form only are shown for both targets as the length form is very close. We see that qualitaive behaviour of the EPI ratios is similar in Be and the "hollow" helium, especially at larger photon energies. This again indicates a passive role of the $1s^2$ core which only serves to shield the excessive charge of the nucleus.

In Fig. 3 we show the double-to-single photoionization cross-sections ratio for He (left panel) and Be (right panel) calculated in the length and velocty gauges. The MCHF-15 and MCHF-13 ground states were used for He and Be, respectively, as indicated in the Table. We note that the length-form calculation with a MCHF-type ground state is not reliable. Our calculation on He [17] with a far more accurate Hylleraas-type ground state agreed well with the MCHF calcualtion in the velocity form. The length form appeared to be significantly off. So, of the two markedly different results in Fig. 3 we favour the velocity form calculation. Qualitatively, and even quantitatively, the

DPI ratio in Be is similar to that in He. A certain scaling should be applied to the photon energy scale as the DPI threshold is markedly different in both these targets (79 eV in He and 27 eV in Be). Again, as in the case of the EPI ratios, the asymptotic DPI ratio for Be is of purely academic interest as the frozen core model loses its validity much earlier than the asympototic ratio can be reached.

B. Triple-differential DPI cross-section

Much more detailed description of the DPI porcess can be achieved when the fully-differential, rather than an integrated, cross-section is measured or calculated. It has been demonstrated very convincingly in the case of He [22]. Although the DPI cross-section ratio in ground state He and Be is quite similar (see Fig. 3) we demonstrate here that the fully resolved TDCS of these two targets are quite different.

We choose the equal energy sharing kinematics $E_1 = E_2$. In this case a simple Gassian ansatz can be applied to the TDCS [23]. We assume the coplanar geometry in which the two photoelectrons are detected in the plane perpendicular to direction of the photon which is fully linearly polarized. The TDCS is then given by the formula [24]:

$$\frac{d\sigma}{d\Omega_1 d\Omega_2 dE_2} = A \exp\left[-4\ln 2 \frac{(\pi - \theta_{12})^2}{\theta_{1/2}^2}\right] (\cos\theta_1 + \cos\theta_2)^2 \qquad (10)$$

Here angles θ_1, θ_2 are counted from the polarization axis of light, the mutual angle is $\theta_{12} = |\theta_1 - \theta_2|$. The magnitude parameter A absorbs the DPI constant and the width parameter $\theta_{1/2}$ defines the width of the Gaussian (10) at the half maximum.

We select the escape energy of the two photoelectrons at 10 eV. In the case of helium this is a widely studied energy partition which we adopt for Be also. While detailed comparison of the TDCS calculated by the CCC and TDCC methods are given by Colgan and Pindzola [9], here we concentrate on an overview.

In Fig. 4 we show the TDCS at the full angular range of the two photoelectrons θ_1, θ_2. The contour plot is used in which the areas of a larger cross-section are indicated by dacker shades of grey. Conventional plots of the TDCS at a fixed escape angle of one of the photoelectrons can be produced as vertical or horizontal cuts across our 3D plots, and are found to be in good agreeement with those obtained from the TDCC method [9].

In our 3D representation the TDCS has a characteristic shape of four islands separated by deep valleys. These valleys are formed due to the nodal lines along which $\cos\theta_1 + \cos\theta_2 = 0$. This forbids the two-electron escape along the straight lines $\theta_1 \pm \theta_2 = \pm 180^\circ$. In addition, the Gaussian term in (10) strongly suppresses the parallel emission at the diagonal $\theta_1 = \theta_2$. The width of the TDCS perpendicular to the diagonal is controlled by the Gaussian parameter $\theta_{1/2}$. Looking at the TDCS plots in Fig. 4 we see that this width is markedly different in Be and He. Indeed, if we fit our calculated TDCS with the Gaussian ansatz (10) we get the width parameters of 90 and 68° for He and Be, respectively. Much smaller Gaussian width in Be means much stronger angular correlations. This difference cannot be attributed to a different photon energy scale. The excess energy of 20 eV takes us relatively further from the DPI threshold in Be than in He. Away from the threshold the width is expected to grow as was confirmed by many studies (see e.g. [25]).

V. CONCLUSIONS

We presented here the integrated and fully-differential cross-sections of the DPI of Be in the frozen-core approximation. This approximation is expected to be valid at photon energies not exceeding the ionization potential of the Be^{2+} ion, i.e. below 180 eV.

We observe that the photon energy dependence of the total ionization-excitation and the double ionization cross-sections in Be resembles qualitatively that of He. The effect of the core is weak. This is illustrated in the Fig. 2 where the cross-section ratios of the single ionization with excitation to the ground state ionization $\sigma_n^+/(\sigma^+ + \sigma^{2+})$ are presented for Be and the "hollow" He $2s^2$ in which the radial orbital $2s$ is made orthogonal to that of the empty $1s$ shell.

Despite similarity of the total cross-sections, the triple differential cross-section (TDCS) in Be and ground state He are quite different. Our calculations at the excess energy of $E = 20$ eV shared equally between the photoelectrons show considerably smaller Gaussian width in Be than in He. This can be interpreted by employing the arguments of Cvejanović and Reddish [26]. They noted that the strength of the angular correlation in the two-electron continuum depends on the time spent by the photoelectrons in the so-called Coulomb zone where they follow the Wannier trajectory. Stronger angular correlation in Be means a larger spatial extend of the Coulomb zone which is not surprizing given a large electron radius of the Be atom. Incidently, a recent non-resonant measurment of the DPI TDCS in Ca [6] also indicates quite a small correltaion width,

probably even smaller than that of Be. A poor statistical accuracy of the Ca data precludes us from making a quantitative estimate.

Our results for both the total and fully-differential cross-sections of the DPI of Be agree well with another non-perturbative calculation by Colgan and Pindzola [9], who used the time-dependent close-coupling approach. Detailed comparison between the two calculations is presented in their paper.

In the future we plan to extend our frozen-core model to a heavier and stronger polarizable Mg and Ca atoms. This would require inclusion of the polarization potential both in the ground and final state.

ACKNOWLEDGMENTS

One of the authors (ASK) wishes to thank the Japan Society for the Promotion of Science for supporting his visit to the Photon Factory. We greatly value many stimulating discussions with Prof. Y. Azuma. The Australian Partnership for Advanced Computing is acknowledged for providing access to the Compaq AlphaServer SC National Facility. The resources of the Maui High Performance Computing Center are also gratefully acknowledged.

REFERENCES

[1] K. J. Ross, J. B. West, and H.-J. Beyer, J. Phys. B **30**(21), L735 (1997).

[2] K. J. Ross, J. B. West, H.-J. Beyer, and A. D. Fanis, J. Phys. B **32**(12), 2927 (1999).

[3] A. K. Kazansky and V. N. Ostrovsky, J. Phys. B **30**(23), L835 (1997).

[4] F. Maulbetsch, I. L. Cooper, and A. S. Dickinson, J. Phys. B **33**(4), L119 (2000).

[5] L. Malegat, F. Citrini, P. Selles, and P. Archirel, J. Phys. B **33**(13), 2409 (2000).

[6] H.-J. Beyer, J. B. West, K. J. Ross, and A. D. Fanis, J. Phys. B **33**(20), L767 (2000).

[7] B. El-Marji, J. P. Doering, J. H. Moore, and M. A. Coplan, Phys. Rev. Lett. **83**(8), 1574 (1999).

[8] Y. Azuma, private communication (2001).

[9] J. Colgan and M. S. Pindzola, Phys. Rev. A (2001).

[10] A. S. Kheifets and I. Bray, Phys. Rev. A **54**(3), R995 (1996).

[11] A. S. Kheifets and I. Bray, Phys. Rev. A **58**(6), 4501 (1998).

[12] K. G. Dyall, I. P. Grant, C. T. Johnson, F. A. Parpia, and E. P. Plummer, Comp. Phys. Commun. **55**, 425 (1989).

[13] A. Dalgarno and A. L. Stewart, Proc. Phys. Soc. London **76**, 49 (1960).

[14] R. C. Forrey, H. R. Sadeghpour, J. Baker, J. D. M. III, and A. Dalgarno, Phys. Rev. A **51**(3), 2112 (1995).

[15] H. W. van der Hart, K. W. Meyer, and C. H. Greene, Phys. Rev. A **57**(5), 3641 (1998).

[16] M. Y. Amusia, *Atomic photoeffect* (Plenum Press, New York, 1990).

[17] A. S. Kheifets and I. Bray, Phys. Rev. A **57**(4), 2590 (1998).

[18] L. V. Chernysheva, N. A. Cherepkov, and V. Radojevic, Comp. Phys. Comm. **11**, 57 (1976).

[19] I. Bray and A. T. Stelbovics, Phys. Rev. Lett. **70**, 746 (1993).

[20] A. S. Kheifets and I. Bray, J. Phys. B **31**(10), L447 (1998).

[21] V. Radojević and W. R. Johnson, Phys. Rev. A **31**(5), 2991 (1985).

[22] J. S. Briggs and V. Schmidt, J. Phys. B **33**(1), R1 (2000).

[23] L. Malegat, P. Selles, and A. Huetz, J. Phys. B **30**(2), 251 (1997).

[24] S. J. Schaphorst, B. Krassing, O. Schwarzkopf, N. Scherer, V. Schmidt, P. Lablanquie, L. Andric, J. Mazeau, and A. Huetz, J. Electron Spectrosc. Relat. Phenom. **76**, 229 (1995).

[25] A. S. Kheifets and I. Bray, Phys. Rev. A **62**(6), 065402 (2000).

[26] S. Cvejanović and T. Reddish, J. Phys. B **33**(21), 4691 (2000).

TABLE I: Asymptotic photoionization cross-section ratios (%) of various two-electron targets

Target	He	He*	Be
Expansion	MCHF15	MCHF5	MCHF13
Orbitals	$l = 0 \ldots 4$	$l = 0 \ldots 2$	$l = 0 \ldots 4$
	$n = 1 \ldots 5$	$n = 2 \ldots 3$	$n = 2 \ldots 5$
R_n^∞ $n = 1$	92.9071		
2	4.7278	91.6062	94.2291
3	0.5970	6.1847	5.0933
4	0.1988	0.4805	0.3961
5	0.0919	0.1483	0.1205
6	0.0504	0.0674	0.0543
7	0.0308	0.0370	0.0296
8	0.0202	0.0228	0.0181
R^∞	1.7587	0.3660	0.3709

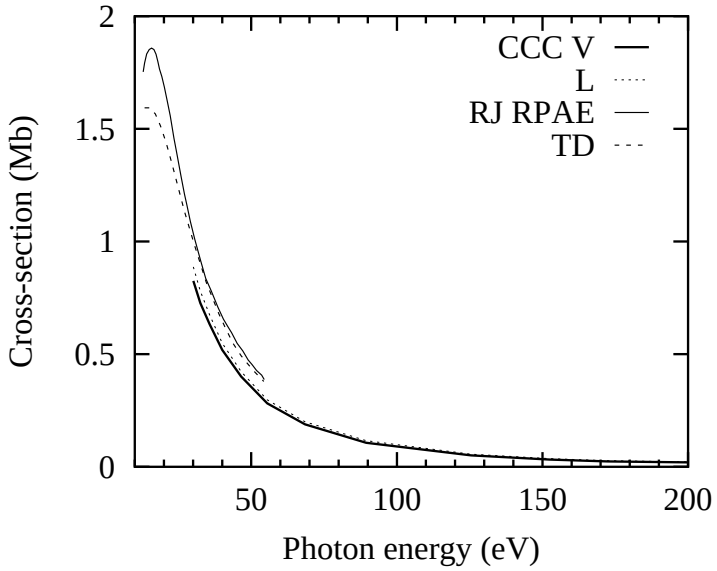

FIG. 1: Photoionization cross-section of Be leaving the Be^+ ion in the ground state. The CCC calculation in the velocity and length gauge is shown by the thick solid and dotted lines, respectivley. The calculations by Radoević and Johnson [21] (labeled as RJ) in the random phase approximation with exchange (RPAE) and the Tamm-Dancoff approximation (TD) are shown by the thin solid and dotted lines, respectively

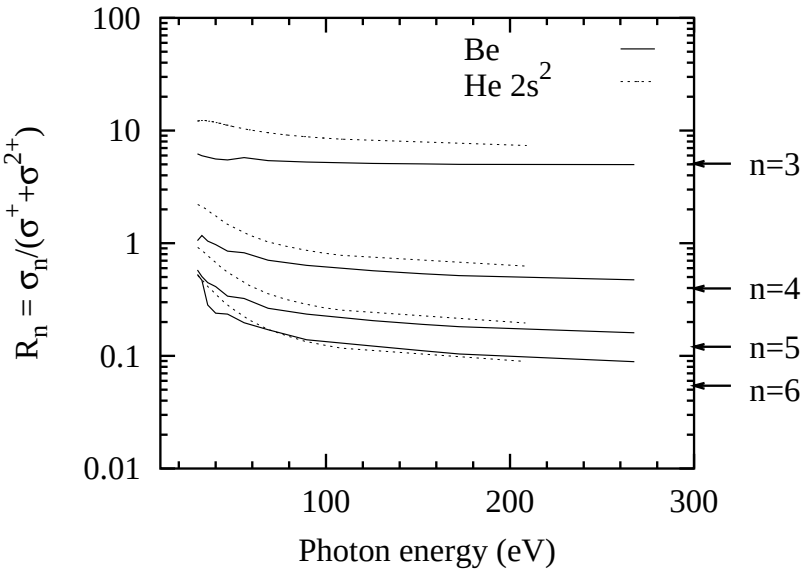

FIG. 2: Velocity gauge calculation of the cross-section ratios of the ionization with excitation to the total photoionization cross-section $R_n = \sigma_n/(\sigma^+ + \sigma^{++})$ in Be (solid line) and the hollow helium (dotted line). The asymptotica ratios R_n^∞ for various n in Be are indicated by arrows.

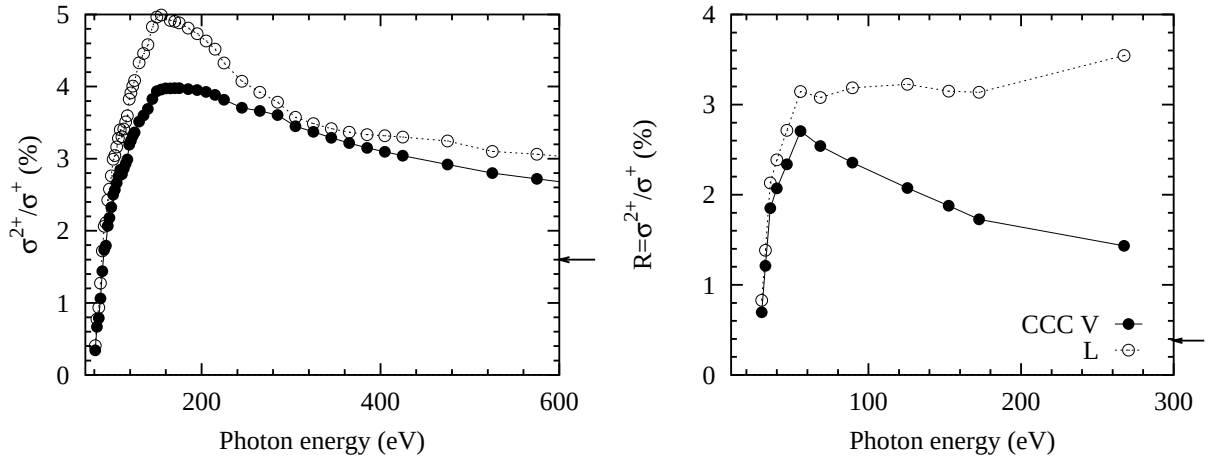

FIG. 3: The double-to-single photoionization cross-section ratio $R = \sigma^{2+}/\sigma^{+}$ in He (left panel) and Be (right panel). Calculations are performed for selected photon energies and results are shown by the closed and open circles for the velocity and length gauges, respectively. The solid lines are to guide the eye. The asymptotic value R^{∞} from the Table is indicated by an arrow.

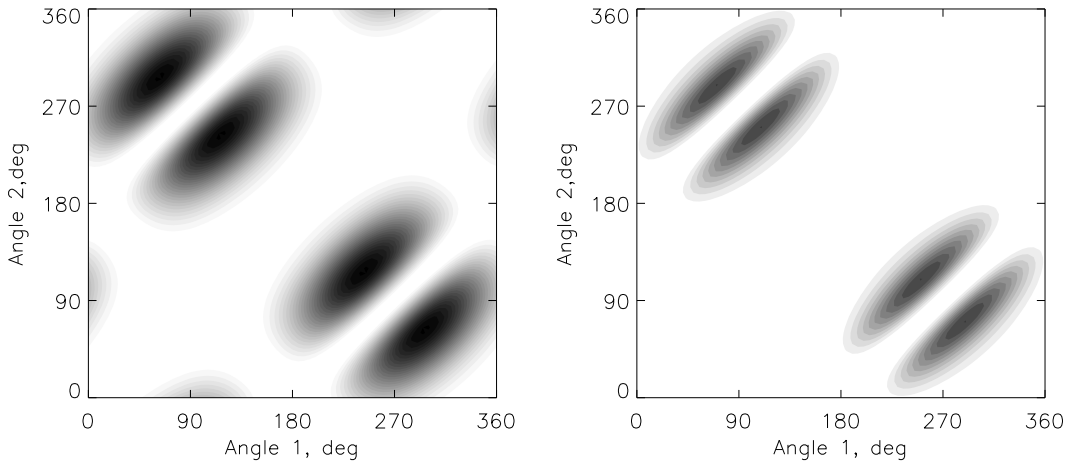

FIG. 4: Contour plots of the TDCS at $E_1 = E_2 = 10$ eV in He (left panel) and Be (right panel). The escape angles of the two photoelectrons θ_1, θ_2 are plotted on the axes, the areals of larger cross-section are indicated by a dacker shade of grey.